

Temperature stabilization of a lab space at 10 mK-level over a day

Dylan Fife,^{1, a)} Dong-Chel Shin,¹ and Vivishek Sudhir^{1, 2}

¹⁾*Department of Mechanical Engineering, Massachusetts Institute of Technology, Cambridge, MA 02139*

²⁾*LIGO Laboratory, Massachusetts Institute of Technology, Cambridge, MA 02139*

(Dated: 11 April 2024)

Temperature fluctuations over long time scales ($\gtrsim 1$ h) are an insidious problem for precision measurements. In optical laboratories, the primary effect of temperature fluctuations is drifts in optical circuits over spatial scales of a few meters and temporal scales extending beyond a few minutes. We present a lab-scale environment temperature control system approaching 10 mK-level temperature instability across a lab for integration times above an hour and extending to a few days. This is achieved by passive isolation of the laboratory space from the building walls using a circulating air gap and an active control system feeding back to heating coils at the outlet of the laboratory HVAC unit. The latter achieves 20 dB suppression of temperature fluctuations across the lab, approaching the limit set by statistical coherence of the temperature field.

I. INTRODUCTION

Long-term temperature drifts have always been the bane of precision measurements, stretching back to pendulum-based timekeeping^{1, 2}, to contemporary atomic clocks^{3–7}. In experiments of this kind, the temperature of the critical subsystem can be stabilized^{3, 8–10}. In contrast, in complex optical experiments spread over a laboratory space, drifts in temperature need to be compensated throughout the laboratory volume. To get a sense of the thermal time scale involved, notice that a 3/16 inch thick, 4 foot \times 10 foot steel top of an optical table acts like a thermal low-pass filter with an approximate cutoff frequency of 10^{-3} Hz (obtained from a simple lumped element heat conduction model¹¹). So, for experiments running for more than 1000 seconds, one would expect that drifts in temperature of the optical table can produce drifts in the alignment of optical circuits built on it. In the worst case, N mirrors each of transverse extension ℓ , spread over an area L^2 , will cause a beam displacement of order $\delta x \approx (NL/\ell)(\partial\ell/\partial T)\delta T$, due to temperature fluctuation δT coupling to the mirror mounts through their thermal expansion coefficient $\partial\ell/\partial T \approx 10^{-5} \text{ K}^{-1}$. For a typically complex optical circuit of 100 1" mirrors over an area of 4 m^2 , this is a worst case drift of $\delta x \approx (100 \text{ cm})(\delta T/1 \text{ K})$.

This work demonstrates temperature stabilization of a laboratory-scale space at the 10 mK level over a time scale of a few days. Significantly better temperature stability has been achieved in volumes more than a million times smaller^{3, 4, 8} by using a sequence of temperature shields and local thermo-electric control^{12, 13}; similar performance has also been reported in meter-scale fully enclosed boxes¹⁴. At the scale of a room, air-conditioning alone is insufficient as that usually targets human comfort and does not usually achieve stability better than a few degrees¹⁵. A solution that has been pursued for precision physics experiments requiring temperature stability over long times is to situate the experiment in a room-scale volume with a large thermal mass — either underground¹⁶, or inside a

mountain¹⁷, which can achieve sub-mK stability¹⁸. These solutions are essentially a large thermal enclosure that is unfit to be used as a general lab space, and they do not generalize beyond specific geographic locations. Indeed, published reports from metrology and standards laboratories around the world^{19–21} show that design and active control can achieve temperature stability around 100 mK; we demonstrate more than an order of magnitude improvement.

II. SETUP AND METHODS

The laboratory room of interest is situated in the basement of the historic main block of the Massachusetts Institute of Technology (MIT). The building, constructed in the early 20th century, has walls facing the outside environment that are several feet thick; however, thermal insulation is compromised by several factors: the presence of a window in that wall, two other walls lacking in thickness, the final wall needing to have a door opening into a corridor, and the fact that MIT's central air handling unit (AHU) varies significantly in air temperature over a day.

Our lab space was designed and renovated for greater temperature stability while simultaneously meeting the competing requirements of reducing acoustic noise and maintaining a cleanroom environment (approximately Class 1000). These requirements are met by a sequence of design choices. The laboratory space is constructed as a room-within-a-room: a few-inch air gap separates the walls of the lab environment from the walls of the building on three sides (see Fig. 1). Of the other surfaces, the one remaining wall opens into a gowning area that partly insulates the lab from the corridor; the ground is anchored to the thermal mass of the several-meter-thick foundation of the MIT main building; and the false ceiling sits below an air gap of 2 feet and contains air handling ducts. The ducts serve air from a custom AHU, which contains a refrigeration system. The cooled air output from it is split in two (see Fig. 1): one part passes through a heater driven by MIT's central hot water

^{a)}Electronic mail: dsfife@mit.edu

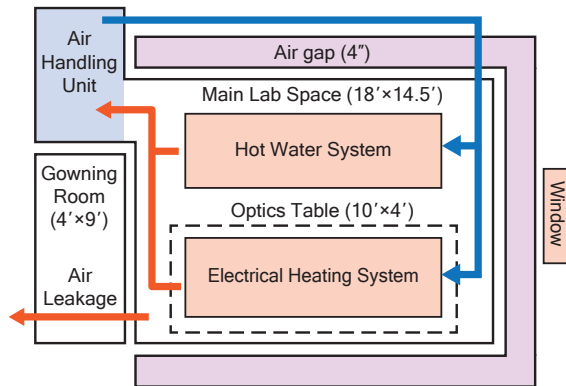


FIG. 1. The lab space layout and the airflow within the space. Red arrows represent the flow of heated air through the lab space, whereas blue arrows represent the flow of cold air through the lab ductwork. The purple air gap is exposed to the temperature fluctuations from the external environment as well as the heated air in the lab and should be at some intermediate temperature.

system and is then fed through HEPA filters onto the part of the lab surrounding the central optical table; the other part passes through electrical coils behind separate HEPA filters over the optical table. (To reduce acoustic noise, careful attention was paid to the geometry of the ducts and air flux through them.) Air from the lab space is recirculated back to the AHU via the air gaps on three sides of the lab. Effectively, this arrangement produces a “Russian doll” thermal insulation of the optical table enclosure: first from the constant recirculation of air behind the lab walls, then from the air heated by the central heaters, and finally, the air falling on the optical table can be heated by the user via an active control system. (The hot water system keeps the human-occupied area of the lab warm when active control of the temperature is off.)

Assuming that the temperature in the optical enclosure is mainly dictated by the temperature of the air flowing into it, we actively stabilize the temperature of this air. A single thermistor (NTE 02-N102-1) in a four-wire configuration is polled at 5 Hz, and its signal is fed back to the electric heaters via a temperature controller (Stanford Research Systems PTC10). A second thermistor — read out by the same controller — is used as an out-of-loop probe. The time series of temperature readings from both probes were recorded in various experiments, to be detailed below, with no human occupation of the lab space. Power spectral densities (PSD) of the long-term temperature time series were estimated using the Welch method²² using Hamming windows whose length spanned 4-14.5 hours ($\sim 2^{16} - 2^{18}$ points) depending on the length of the experimental run, an overlap of 50%, and linear detrending to avoid bias in the lowest frequency bins of the PSD estimates. In order to quantify the effect of long-term drifts, we also investigate the modified Allan

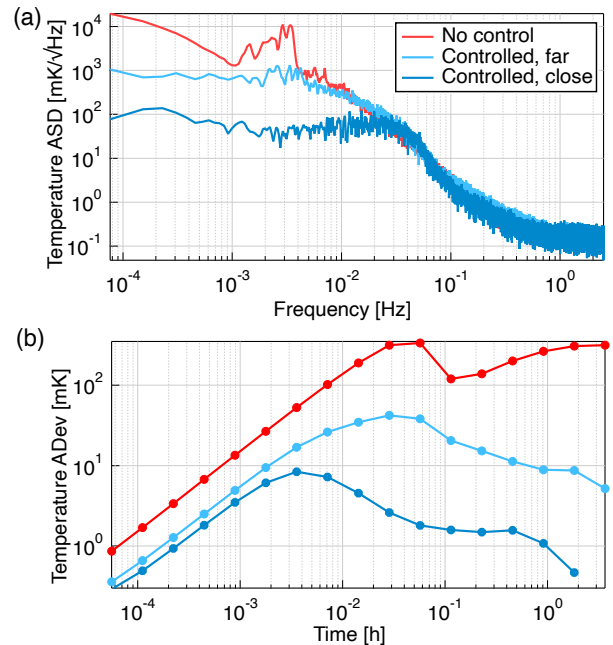


FIG. 2. (a) shows the ASD of the free-running temperature (red), and when the temperature is controlled (blue); dark blue shows the temperature measured a few mm away from the sensor used for control, while light blue shows the temperature measured 2.35 m away from the sensor. (b) shows the modified Allan deviation of the same time series underlying the data in panel (a); colors are identical to panel (a).

deviation of the temperature data²³.

III. RESULTS

To ascertain the performance and effect of the passive and active temperature stability of the laboratory space, several measurements were performed. First, we measured the temperature fluctuations with and without the active control system, with the two sensors placed next to each other. Second, the sensors were placed across the room from each other to quantify the effect of control over large spatial scales. Third, a laser beam was bounced across the length of the optical table to measure the effect of temperature stability on the geometric stability of the beam path. In the following, we detail the results of these investigations.

In the first experiment, the controller sent a constant reference voltage to the heater, but the feedback loop was not closed. In essence, we measure the passive stability of temperature in the lab space without active feedback control. Data is recorded continually over three days, and its amplitude spectral density (ASD) and modified Allan deviation are shown in red in Fig. 2. The peaks in the temperature spectrum around frequency $f \approx (5 \text{ min})^{-1}$ corresponds to the typical time over which the AHU takes in air from the outside. However, passive isolation

already suffices to keep the temperature stable to within ~ 200 mK as apparent from the Allan deviation.

Next, active feedback based on a single thermistor is turned on, and a second (out-of-loop) thermistor is placed in its vicinity as a witness of temperature. Given the hours-long response time of the temperature in the room, we employ the relay tuning feature of the controller (which sends a series of steps into the heater and observes the response on the thermistor to tune a PID filter). The dark blue lines in Fig. 2 show the data from such an experiment. Apparently, the feedback loop has a unity-gain frequency of $\sim 2 \cdot 10^{-2}$ Hz, which suffices to affect a 100-fold reduction in the ASD. As evident from the Allan deviation, active control succeeds in attaining a stability less than 1 mK over three days *in the vicinity of the sensing thermistor*.

Clearly, temperature fluctuations faster than 10^{-2} Hz ≈ 100 s are not suppressed by active control. This is largely due to the delay in the feedback loop arising from the slow response of the heaters and the concomitant limitation in closed-loop stability that curtails bandwidth. In any case, smaller parts of an experiment can be isolated from such high-frequency temperature fluctuations by thermalizing them with a large thermal mass, which acts like a low-pass filter. The thermistor, by comparison, has a lower thermal mass than most optical components. As such, any optical component is unlikely to be susceptible to temperature fluctuating faster than 100s.

In a second experiment, to quantify the efficacy of the temperature control over the spatial scale of the lab, we move the out-of-loop sensor to a distance of 2.35 m from the in-loop sensor. The light blue traces in Fig. 2 show the results. There are noticeable gains in temperature fluctuations around the peak, but the temperature across the lab is more noisy compared to the temperature in the vicinity of the in-loop sensor. Even so, within about an hour, the temperature across the lab is stable to within 10 mK, as shown by the Allan deviation.

We expect that much of the residual noise across the lab is not coherent across the lab space, and so our control system, which only has one degree of freedom, cannot compensate for uneven temperature gradients. To ascertain the limitation posed by the incoherence of the temperature field across the lab, consider the temperature fluctuations T_1 and T_2 at any two locations. The power spectral density of their difference $S_{T_1-T_2}$ is zero if and only if the two random processes have identical trajectories in any given sample. This quantity is, however lower-bounded by the (magnitude of the) coherence $C_{T_1 T_2} \equiv |S_{T_1 T_2}| / \sqrt{S_{T_1} S_{T_2}}$, as follows:

$$\begin{aligned} S_{T_1-T_2} &= S_{T_1} + S_{T_2} - 2 \operatorname{Re} S_{T_1 T_2} \\ &\geq 2\sqrt{S_{T_1} S_{T_2}} - 2|S_{T_1 T_2}| \cos(\arg S_{T_1 T_2}) \quad (1) \\ &\geq 2\sqrt{S_{T_1} S_{T_2}}(1 - C_{T_1 T_2}). \end{aligned}$$

Thus, $S_{T_1-T_2} = 0$ if and only if the coherence attains its maximum value $C_{T_1 T_2} = 1$, i.e. iff. the temperature field is perfectly coherent across the two locations. (The

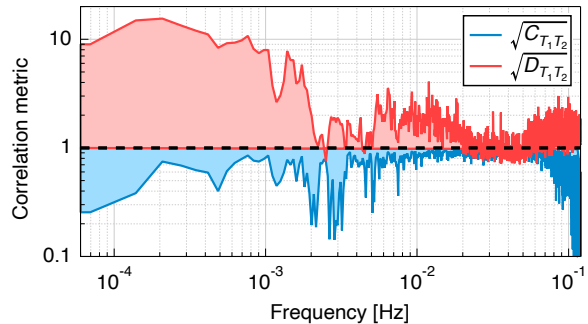


FIG. 3. Blue shows the coherence $C_{T_1 T_2}$ between the temperatures measured by the two sensors when they are separated by 2.35 m. The two temperatures lack coherence at the lowest frequencies. Red shows the figure of merit $D_{T_1 T_2}$ defined in Eq. (2). The excess value of D over unity is consistent with the degree of incoherence.

fact that $C_{T_1 T_2} \leq 1$ follows from the Cauchy-Schwarz inequality.) Alternatively, if the temperature across the two locations is not perfectly coherent (i.e. $C_{T_1 T_2} \neq 1$), any attempt to control one based on a measurement of the other will not be perfect, and the lack of imperfection due to this effect can be quantified by the figure of merit,

$$D_{T_1 T_2} \equiv \frac{S_{T_1-T_2}}{2\sqrt{S_{T_1} S_{T_2}}(1 - C_{T_1 T_2})} \geq 1. \quad (2)$$

Figure 3 shows this figure of merit in red, and the coherence $C_{T_1 T_2}$ in blue. $D_{T_1 T_2}$ was in excess above its realistic lower bound of unity by a factor of 10, which is commensurate with the drop in coherence (from its upper bound of unity) by roughly the same factor. This shows that the current temperature control system approaches the limit set by the statistical coherence of the temperature field, with only marginal improvements possible by tuning the controller.

Our ultimate interest is in the effect of temperature drift as it pertains to drifts in optical circuits in the lab. To characterize this effect, we measured the angular deflection of a laser beam traversing the perimeter of our optical table. A beam was derived from a 1064 nm laser and reflected off of 5 mirror mounts (Thorlabs KM100) around the table and measured using a quadrant photodetector (QPD). In order to cancel beam pointing noise intrinsic to the laser, a second beam was derived using a beam-splitter and measured on another QPD co-located with the first QPD after the beam traversed the shortest possible path between the beam-splitter and the QPD. The subtracted photocurrent from the two QPDs (which largely eliminated the common pointing noise of the two beams) was used as a proxy of the angular deflection of the beam traversing the perimeter of the optical table. Figure 4 depicts the resulting signal calibrated in angle units, with and without the temperature control. It is apparent that stabilizing the temperature of the laboratory space noticeably decreases low-frequency drifts in the laser beam's deflection.

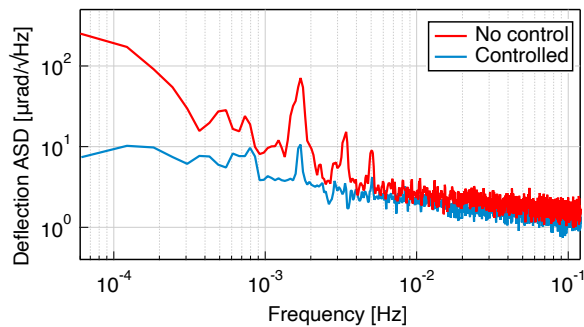


FIG. 4. ASD of the angular deflection of a laser beam traversing a 6 m path along an optical table inside the lab space. Active control of the temperature leads to an order-of-magnitude reduction in drift down to $10 \mu\text{rad}/\sqrt{\text{Hz}}$.

IV. CONCLUSION

We designed and commissioned a laboratory space for precision measurements that is temperature-stable at the $\sim 10 \text{ mK}$ -level after an hour of averaging and over day-long time scales. This level of stability is about an order of magnitude improvement over laboratory scale temperature control demonstrated previously^{19–21}, and is achieved by a combination of passive isolation and active control of the entire lab space. Active temperature control suppresses the passively isolated temperature by a 100-fold. The achieved temperature stability manifests as an order of magnitude improvement in the angular drift of a laser beam traversing a $\sim 6 \text{ m}$ path around an optical table, at the level of $10 \mu\text{rad}/\sqrt{\text{Hz}}$. Since the scheme presented here is independent of the specific use-case or geographical location of the lab, it can be transplanted into the design of any precision measurement lab.

Importantly, the performance of our single degree of freedom controller approaches the limit set by the statistical coherence of the temperature field being controlled. Thus, significant improvement can only be achieved by techniques such as sensor fusion of a network of temperature sensors and spatially localized actuation.

DATA AVAILABILITY

The data that support the findings of this study are available from the corresponding author upon reasonable request.

ACKNOWLEDGEMENTS

The design and construction of the lab was made possible by the generous support of the MIT School of Engineering and the Department of Mechanical Engineering. We also thank Pierre Lermusiaux, Jon Keller, Alireza Heidari, Doug Bell, Dorian Alba, William Mackie, Thomas

Graffeo, and Alex Farrell.

- ¹J. Jackson, “Shortt Clocks and the Earth’s Rotation,” *Monthly Notices of the Royal Astronomical Society* **89**, 239 (1929).
- ²R. J. Matthys, *Accurate Clock Pendulums* (Oxford University Press, 2004).
- ³T. Middelmann, S. Falke, C. Lisdat, and U. Sterr, “High Accuracy Correction of Blackbody Radiation Shift in an Optical Lattice Clock,” *Physical Review Letters* **109**, 263004 (2012).
- ⁴B. J. Bloom, T. L. Nicholson, J. R. Williams, S. L. Campbell, M. Bishof, X. Zhang, W. Zhang, S. L. Bromley, and J. Ye, “An optical lattice clock with accuracy and stability at the 10^{-18} level,” *Nature* **506**, 71–75 (2014).
- ⁵D. G. Enzer, W. A. Diener, D. W. Murphy, S. R. Rao, and R. L. Tjoelker, “Drifts and Environmental Disturbances in Atomic Clock Subsystems: Quantifying Local Oscillator, Control Loop, and Ion Resonance Interactions,” *IEEE Transactions on Ultrasonics, Ferroelectrics, and Frequency Control* **64**, 623–633 (2017).
- ⁶E. A. Burt, J. D. Prestage, R. L. Tjoelker, D. G. Enzer, D. Kuang, D. W. Murphy, D. E. Robison, J. M. Seubert, R. T. Wang, and T. A. Ely, “Demonstration of a trapped-ion atomic clock in space,” *Nature* **595**, 43–47 (2021).
- ⁷A. Aeppli, K. Kim, W. Warfield, M. S. Safronova, and J. Ye, “A clock with 8×10^{-19} systematic uncertainty,” *arXiv:2403.10664* (2024).
- ⁸S. Micalizio, A. Godone, F. Levi, and C. Calosso, “Medium-long term frequency stability of pulsed vapor cell clocks,” *IEEE Transactions on Ultrasonics, Ferroelectrics, and Frequency Control* **57**, 1524–1534 (2010).
- ⁹R. Sugihara and R. K. Gupta, “Clock Synchronization with Deterministic Accuracy Guarantee,” in *Wireless Sensor Networks*, edited by P. J. Marrón and K. Whitehouse (Springer, 2011) pp. 130–146.
- ¹⁰R. Vicarini, M. Abdel Hafiz, V. Maurice, N. Passilly, E. Kroemer, L. Ribetto, V. Gaff, C. Gorecki, S. Galliou, and R. Boudot, “Mitigation of Temperature-Induced Light-Shift Effects in Miniaturized Atomic Clocks,” *IEEE Transactions on Ultrasonics, Ferroelectrics, and Frequency Control* **66**, 1962–1967 (2019).
- ¹¹C. H. Forsberg, “Chapter 4 - Unsteady conduction,” in *Heat Transfer Principles and Applications*, edited by C. H. Forsberg (Academic Press, 2021) pp. 121–162.
- ¹²B. Kocjan, K. Krawczyk, L. Snopek, R. Jasinski, and E. Dudek, “Temperature Chamber with Precise Temperature Stability,” in *2018 Conference on Precision Electromagnetic Measurements (CPEM 2018)* (2018) pp. 1–2, iSSN: 2160-0171.
- ¹³G. Andria, G. Cavone, C. G. C. Carducci, M. Spadavecchia, and A. Trotta, “A pwm temperature controller for thermoelectric generator characterization,” in *2016 IEEE Metrology for Aerospace (MetroAeroSpace)* (2016) pp. 291–296.
- ¹⁴P. Egan and J. A. Stone, “Temperature stabilization system with millikelvin gradients for air refractometry measurements below the 10^{-8} level,” *NCSLI Measure* **6**, 40 (2011).
- ¹⁵A. Ghahramani, K. Zhang, K. Dutta, Z. Yang, and B. Becerik-Gerber, “Energy savings from temperature setpoints and dead-band: Quantifying the influence of building and system properties on savings,” *Applied Energy* **165**, 930–942 (2016).
- ¹⁶P. G. Roll, R. Krotkov, and R. H. Dicke, “The equivalence of inertial and passive gravitational mass,” *Annals of Physics* **26**, 442–517 (1964).
- ¹⁷T. Brack, B. Zybach, F. Balabdaoui, S. Kaufmann, F. Palmegiano, J.-C. Tomasina, S. Blunier, D. Scheiwiller, J. Fankhauser, and J. Dual, “Dynamic measurement of gravitational coupling between resonating beams in the hertz regime,” *Nature Physics* **18**, 952–957 (2022).
- ¹⁸N. Krishnan, S. Pereira, and A. Vaidyanathan, “Generating sub-millidegree thermal stability over large volumes for precision experiments,” in *Proceedings of Science*, Vol. 353 (2020) p. 59.
- ¹⁹D. Braudaway, “A new state-of-the-art standards facility,” *IEEE Transactions on Instrumentation and Measurement* **41**, 1020–1022 (1992).

- ²⁰A. Soueid, H. Amick, and T. Zsirai, “Addressing the environmental challenges of the NIST Advanced Measurement Laboratory,” in *Buildings for Nanoscale Research and Beyond*, Vol. 5933 (SPIE, 2005) pp. 169–181.
- ²¹A. Lassila, M. Kari, H. Koivula, U. Koivula, J. Kortström, E. Leinonen, J. Manninen, J. Manssila, T. Mansten, T. Meriläinen, J. Muttilainen, J. Nissilä, R. Nyblom, K. Riski, J. Sarilo, and H. Isotalo, “Design and performance of an advanced metrology building for MIKES,” *Measurement* **44**, 399–425 (2011).
- ²²P. Welch, “The use of fast fourier transform for the estimation of power spectra: A method based on time averaging over short, modified periodograms,” *IEEE Transactions on Audio and Electroacoustics* **15**, 70–73 (1967).
- ²³W. Riley and D. A. Howe, “*Handbook of Frequency Stability Analysis*,” Tech. Rep. (National Institute of Standards and Technology, 2008).